Geochemistry, Geophysics, Geosystems

Supporting Information for

Variability of Natural Methane Bubble Release at Southern Hydrate Ridge

Yann Marcon[1], Deborah Kelley[2], Blair Thornton[4,5], Dana Manalang[3], Gerhard Bohrmann[1]

[1]MARUM – Center for Marine Environmental Sciences and Department of Geosciences, University of Bremen, Bremen, D-28359, Germany.

[2]School of Oceanography, University of Washington, Seattle, USA.

[3]Applied Physics Lab, University of Washington, Seattle, USA.

[4]Centre for In situ and Remote Intelligent Sensing, Faculty of Engineering and Physical Sciences, University of Southampton, Hampshire, UK.

[5]Institute of Industrial Science, The University of Tokyo, Tokyo, Japan.

Contents of this file

Additional Supporting Information (Files uploaded separately)

Introduction

The supporting information given here includes fifteen figures, one table, three datasets and four movies. Figure S1 shows the recording times of most instruments used in this work. Figure S2 illustrates the bubble detection workflow of the MATLAB script provided in Dataset S1. Figures S3 and S4 show the timeseries data from the CTD and the tsunami pressure sensor. Figure S5 shows the SHROS magnitude data of individual plume clusters from 19 October to 8 November 2018. Figure S6 and S7 show the power spectral density of the SHROS data for the main plume clusters. Figure S8 shows the bubble count from the automated analysis of the CAMDSB103 camera for the entire duration of the SHROS monitoring period. Figure S9 illustrates how tidal bottom currents deflect bubble plumes and influence the quality of the

detection of bubble-induced upwelling flows by the ADCP. Figures S10 to S13 show bottom motion data recorded by the ocean bottom seismometers. Figures S14 and S15 show the wave height data recorded by the closest surface buoy along with the bottom pressure data. Table S1 contains the operation log of the SHROS instrument including the downtimes and the main settings used. Dataset S1 is a zip file containing the MATLAB script used to count bubbles in the CAMDSB103 images. Dataset S2 is a zip file containing a color plot showing the ADCP current velocities recorded by the ADCP for each calendar month between 29 June 2018 and 29 February 2020. Dataset S3 is an Excel file containing the results of the analysis of the 4K video sequences (CAMPIA101 camera) in terms of plume counts and bubble rise velocities. Movies S1 and S2 compile the timestamped scan images produced from the SHROS and the single-beam scanning-sonar (QNTSRA101) data. Movies S3 and S4 compile the still images acquired at 30-minutes intervals at Einstein's Grotto (CAMDSB103 camera) and Summit-A (CAMPIA101 camera). These movies allow for a better visualization of temporal changes than the still images.

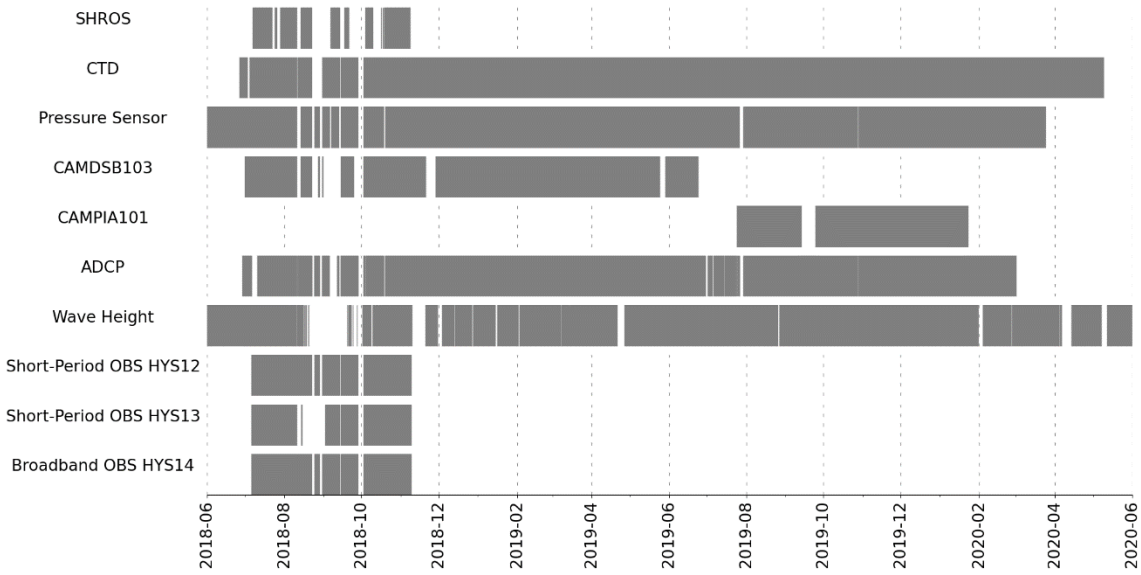

Figure S1. Gantt chart showing the recording times of each instrument used in this work (except the scanning-sonar) from 1 June 2018 to 1 June 2020. For the ocean bottom seismometers (OBS), the chart shows the recording times corresponding to the data used in this work, i.e. only for the monitoring period of the SHROS from 6 July 2018 to 8 November 2018.

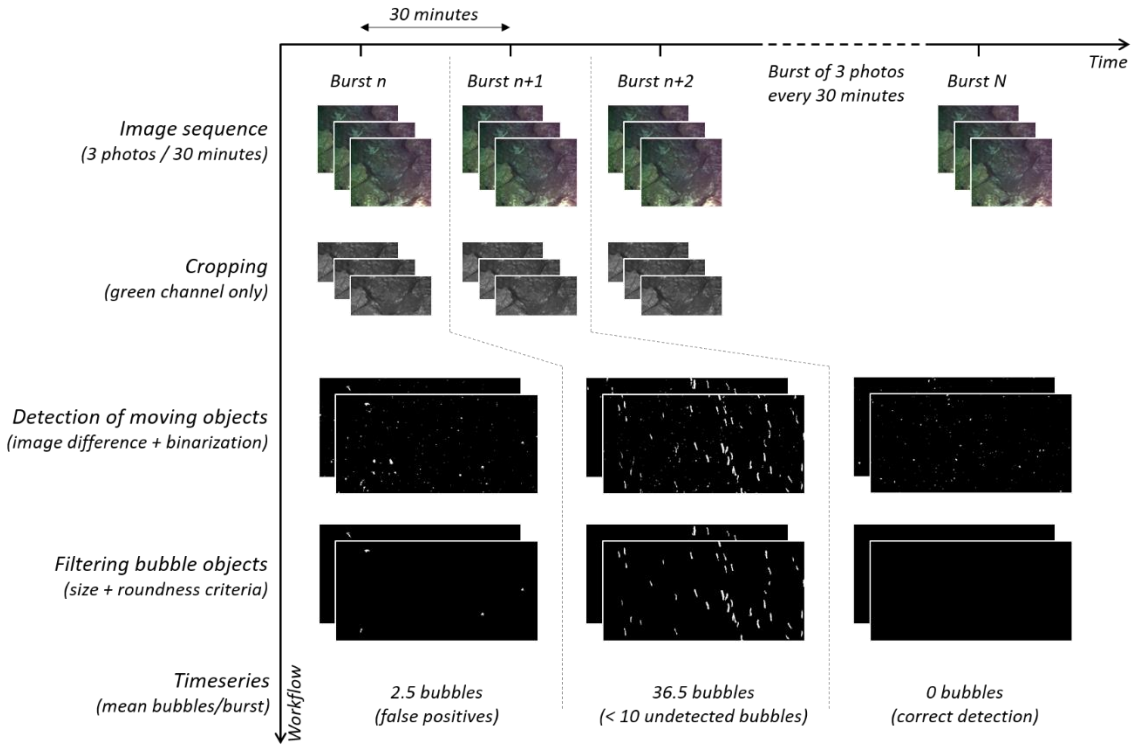

Figure S2. Workflow of the bubble detection method used to count the number of bubbles on the CAMDSB103 camera images. The camera took bursts of 3 images within one second every 30 minutes. The workflow calculates the average number of bubbles for each burst and returns one value per burst. Firstly, images are cropped to eliminate parts of the image that would impair the bubble detection (e.g. the bottom, where mobile benthic fauna is common). Cropping is done on the green channel, which is the least noisy. Next, consecutive images within a same burst are subtracted to remove the background, and binarized using an empirical intensity threshold to identify moving objects. Finally, moving objects are filtered based on their size and roundness (bubbles on the CAMDSB103 images are elongated and have low roundness values). The entire workflow is done by a MATLAB script (Dataset S1).

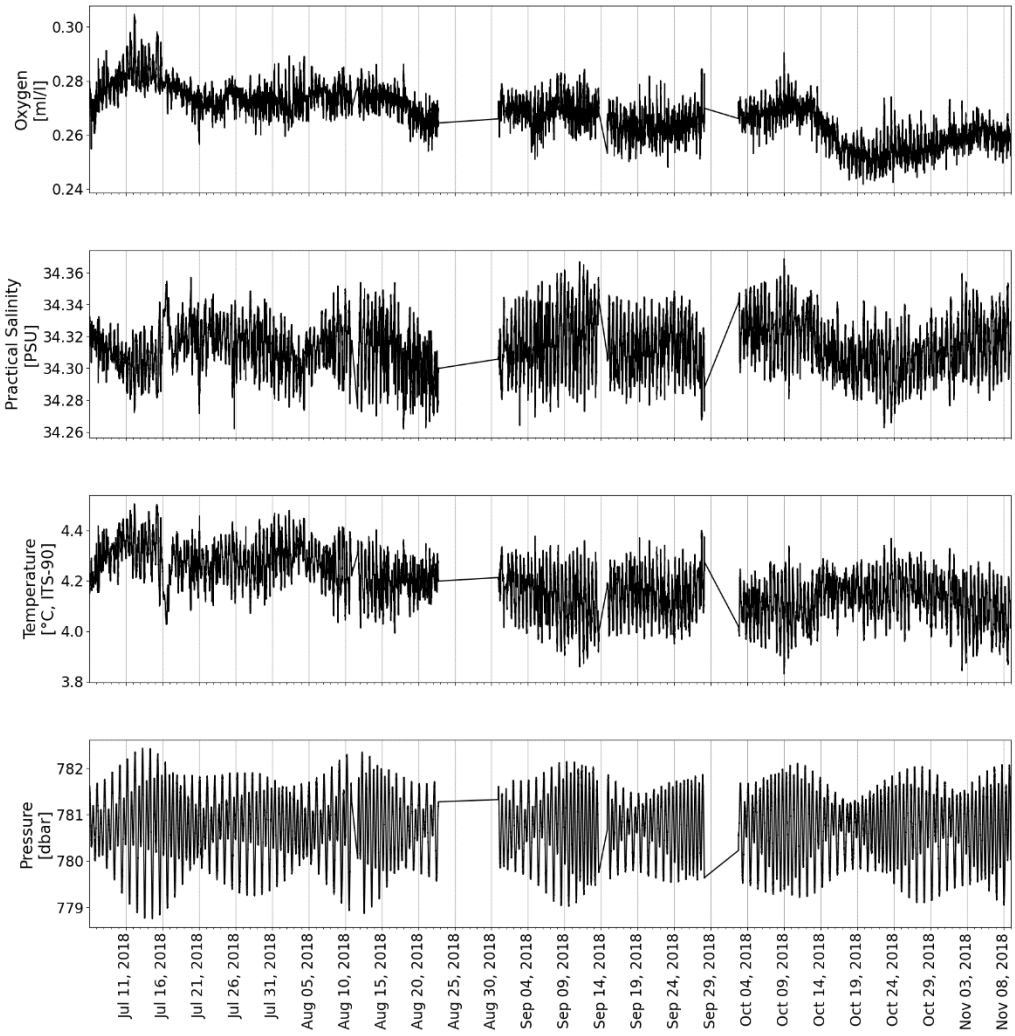

Figure S3. Pressure, temperature, salinity and oxygen timeseries recorded by the cabled CTD instrument at the SHR summit during the SHROS monitoring period (from 6 July to 8 November 2018).

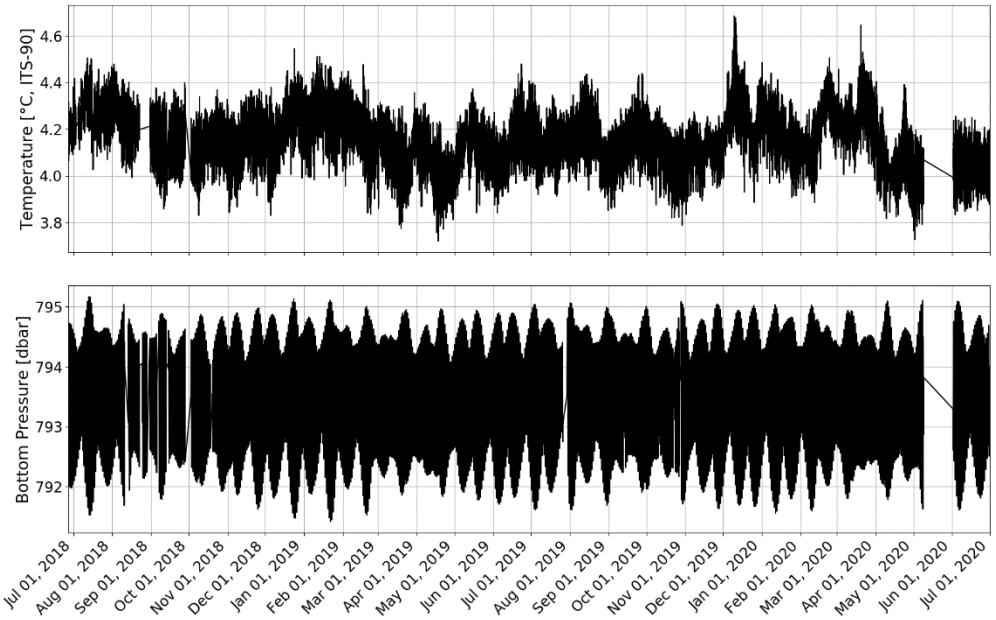

Figure S4. Bottom pressure and bottom water temperature at the SHR summit over almost two years between June 2018 and June 2020. The bottom pressure data were recorded by the tsunami pressure sensor and the temperature data were recorded by the cabled CTD instrument.

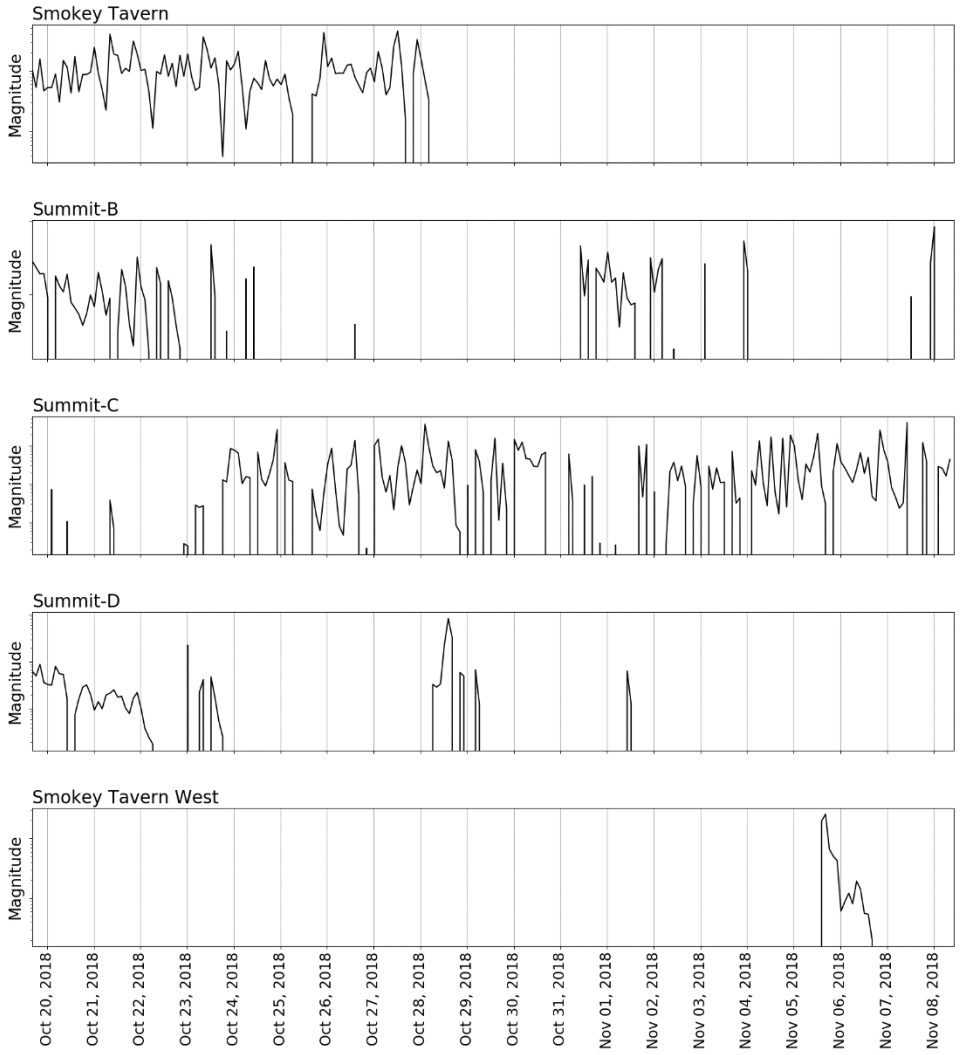

Figure S5. SHROS magnitude data from 19 October to 8 November 2018 for individual plume clusters. Einstein's Grotto and Summit-A are not shown because of the restricted 245° scanning sector of the SHROS after 10 October 2018. Far NE, Far S, Summit South, and Summit SW are not shown because they were inactive over this period. The vertical axis is logarithmic to facilitate visualization of low magnitude variations. Absolute magnitude values cannot be compared between the clusters due to a distance bias (see text) and are not shown.

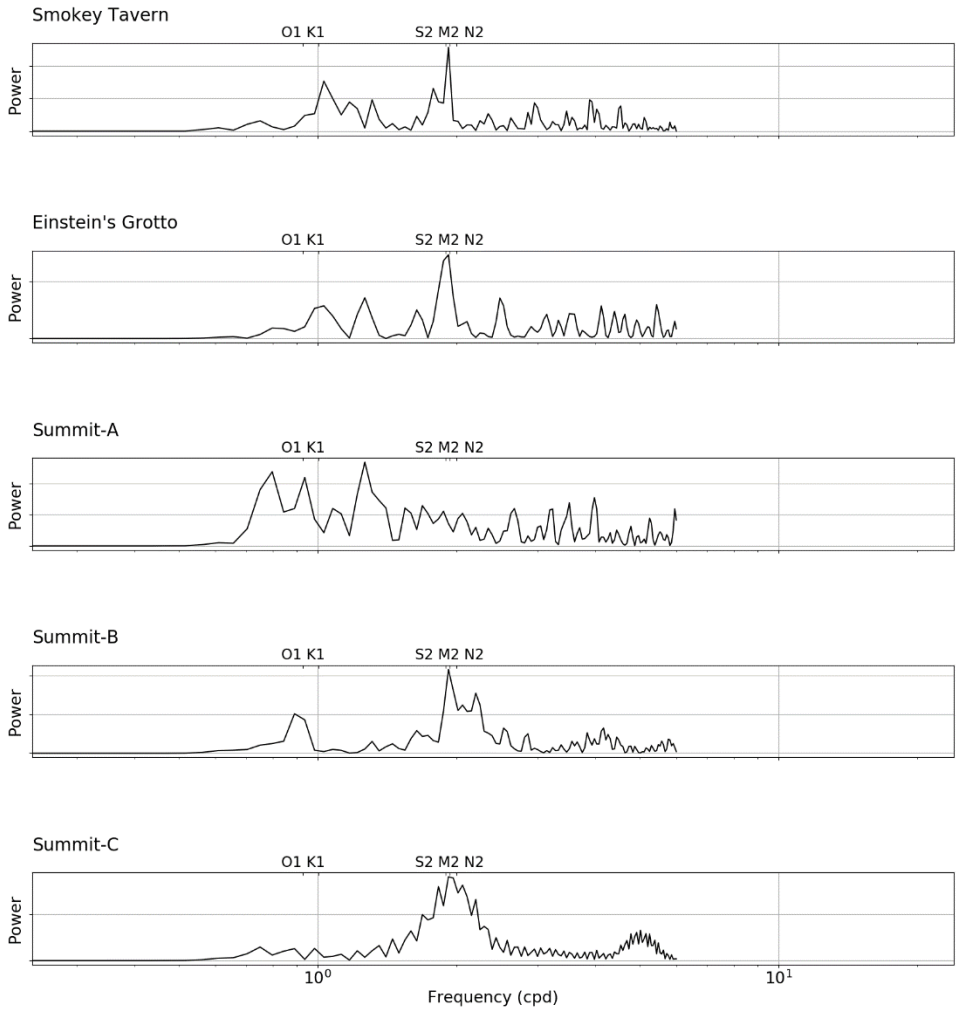

Figure S6. Power spectral density plots of the SHROS data for the most active plume clusters (for the 6-22 July 2018 monitoring period). The semi-diurnal constituents of the tide are clearly present in all plots except at Summit-A. For readability, the frequency units are shown in cycles per day (cpd), and the diurnal (O1, K1) and semi-diurnal (M2, N2, S2) harmonic constituents of the local tide are reported at the top of each plot.

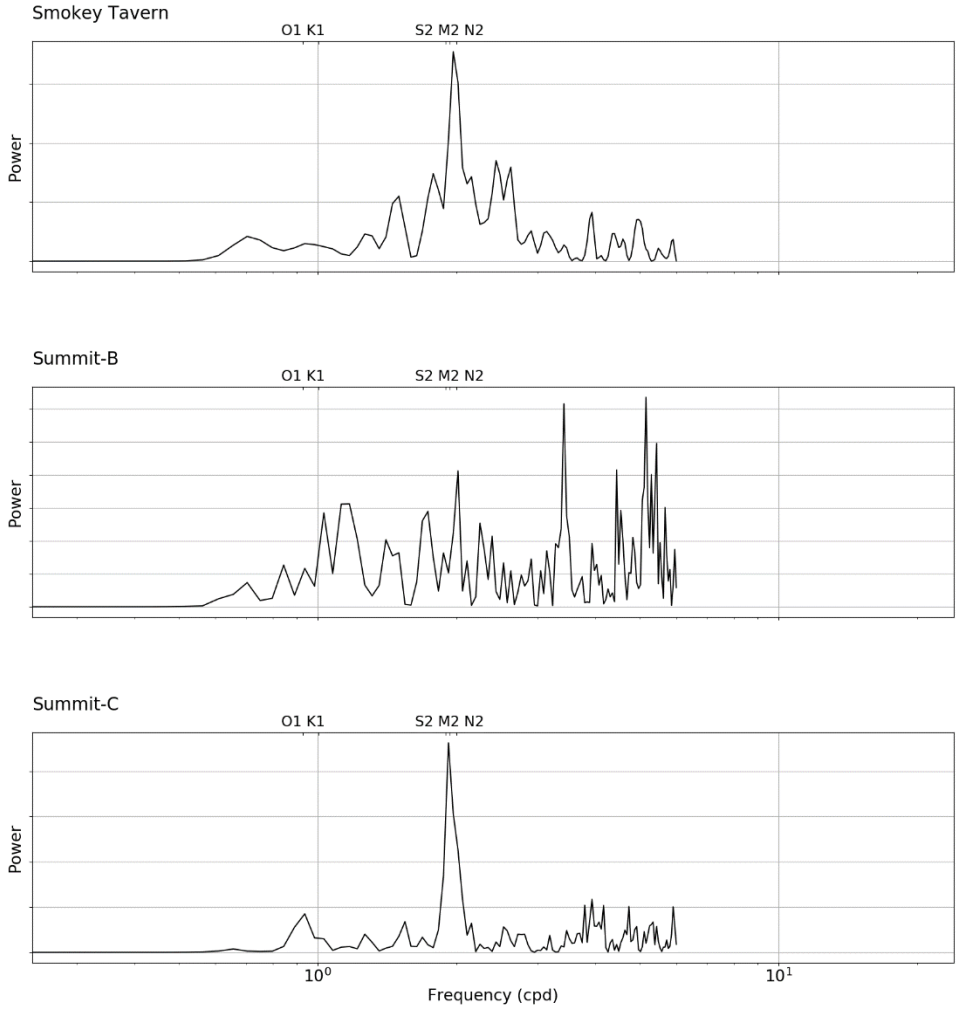

Figure S7. Power spectral density plots of the SHROS data for the most active plume clusters (for the 19 October to 8 November 2018 monitoring period). The semi-diurnal constituents of the tide are present in all plots. For readability, the frequency units are shown in cycles per day (cpd), and the diurnal (O1, K1) and semi-diurnal (M2, N2, S2) harmonic constituents of the local tide are reported at the top of each plot.

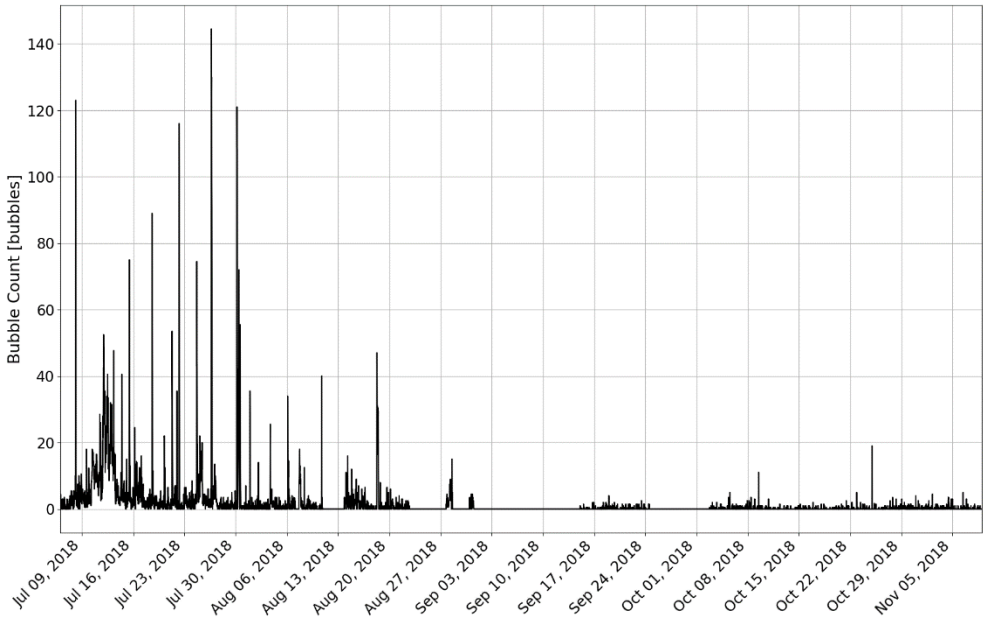

Figure S8. Bubble counts at Einstein's Grotto from 6 July to 8 November 2018 resulting from the automated analysis of the CAMDSB103 images. The main bubble release outlet moved out of the camera field of view, which explains the low bubble count after 18 August 2018. Bubble counts lower than about 5 are below the accuracy of the counting method and might be caused by false detection of bubble objects.

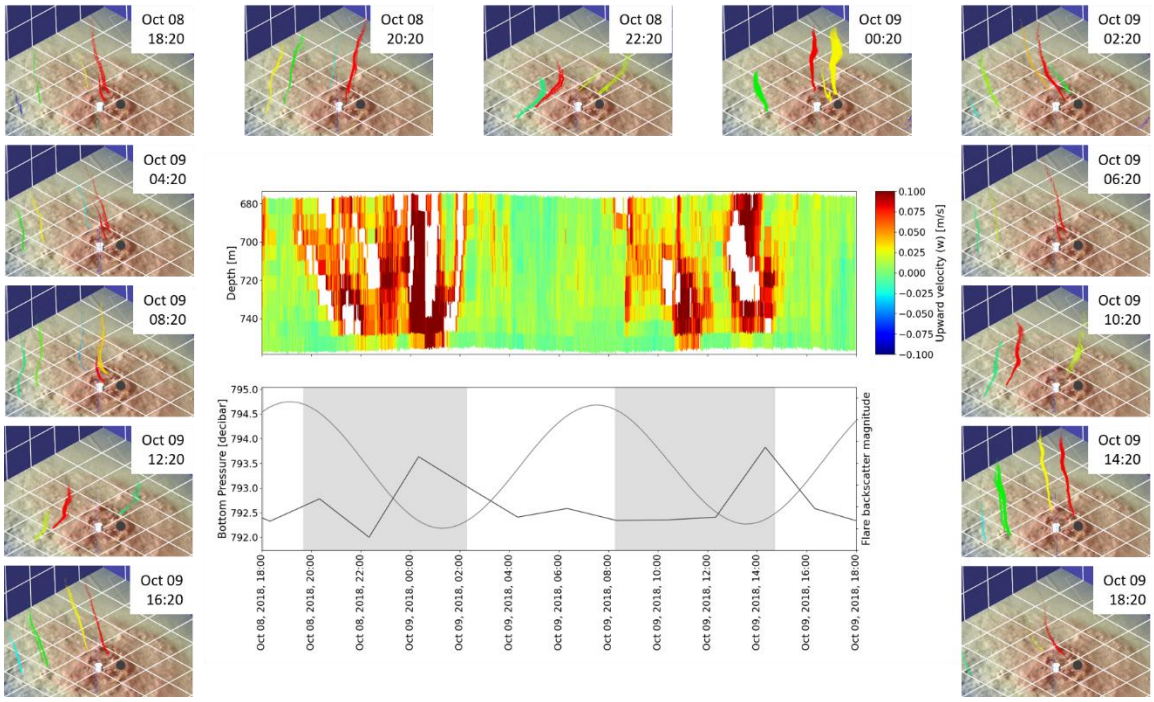

Figure S9. Illustration of the ADCP bias when analyzing gas emission variability. The central color plot shows the vertical velocities measured by the ADCP for the bottom 100 m of the water column over two tidal cycles (the blanked areas are caused by the presence of bubble plumes crossing the ADCP beams). The bottom plot shows the bottom pressure and the SHROS backscatter magnitude (dimensionless). The grey bands indicate the timing of the bubble-induced upward flows detected by the ADCP. The 3D images around the plots show gas emissions detected by the SHROS (after post-processing) every 2 hours over the same tidal cycles (the white cylinder and the grey dot mark the respective locations of the SHROS and the ADCP, the white lines are 62.5 m apart). The ADCP shows semidiurnal upwelling flows with velocities exceeding 2.5 cm/s and coincident with the presence of data blanking (caused by bubbles), which occur during decreasing tide, apparently supporting the idea of tidally-controlled gas emissions. However, the SHROS data also show that, while gas emissions tend to be larger during ebb and low tide, bubble release actually does not stop during flood tide, but is deflected away from the ADCP beams. The ADCP data are biased in that they record bubble occurrence and upwelling flows only when the bottom currents do not deflect bubble plumes away from the ADCP beams. This bias imprints a semi-diurnal periodicity to the vertical velocities measured by the ADCP.

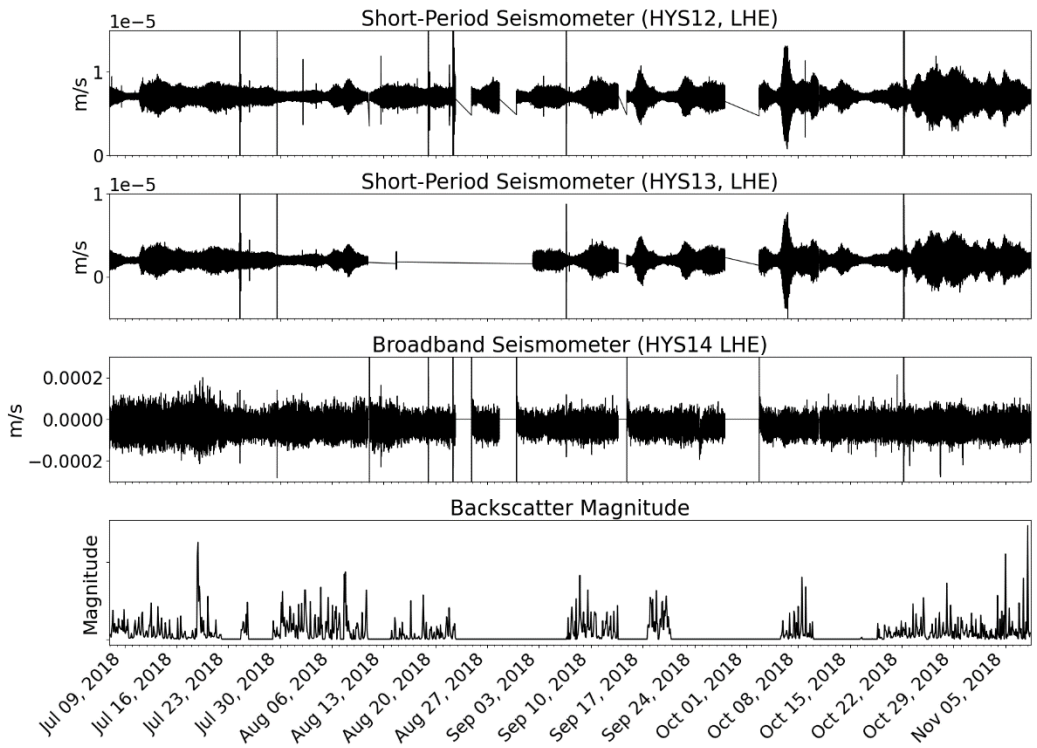

Figure S10. Bottom movements recorded by two short-period seismometers (HYS12 and HYS13) and one broadband seismometer (HYS14) between 6 July 2018 and 8 November 2018. The tremor with the largest amplitude that was recorded during the SHROS monitoring period occurred on 22 October 2018 and was recorded by all three seismometers. The top three plots show the long period LHE channel (1 Hz sample rate) of the three seismometers. The bottom plot shows the normalized SHROS backscatter magnitude for the entire monitoring period including the data gaps; the relative magnitude cannot be compared between individual segments of the timeseries (separated by data gaps) because the sonar settings have changed several times during the monitoring period (Table S1).

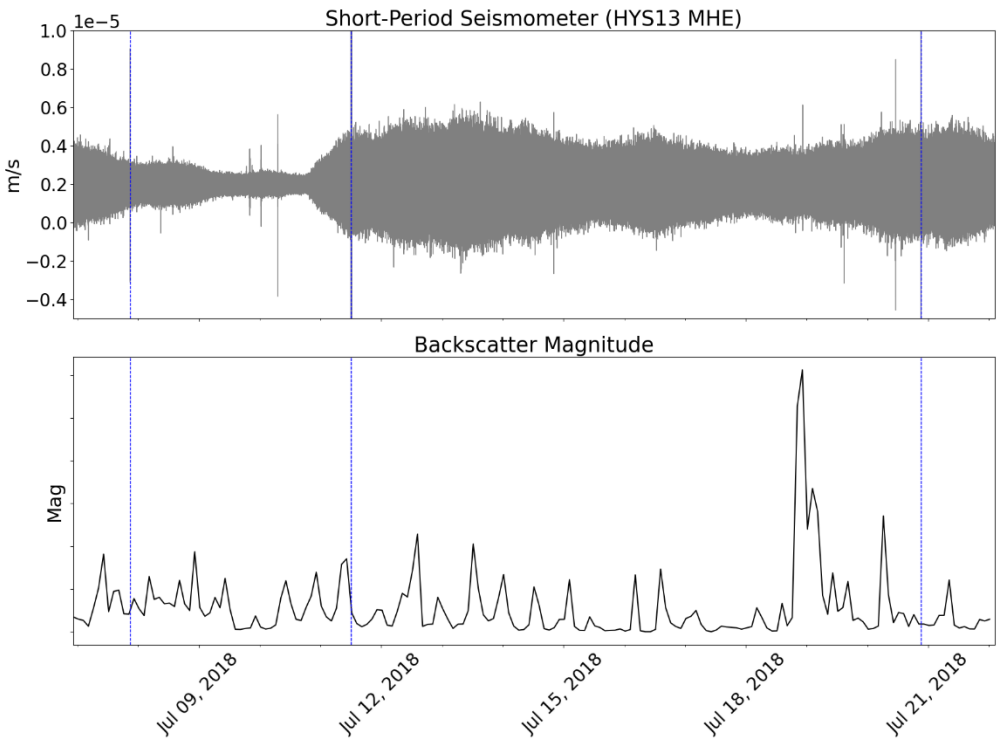

Figure S11. Bottom movements recorded by a short-period seismometer (top) and SHROS magnitude data (bottom) between 6 July and 22 July 2018. The blue lines show when high-amplitude short duration events occurred. The detected SDEs did not coincide with heightened bubble release. The seismic plot shows the mid period MHE channel (8 Hz sample rate).

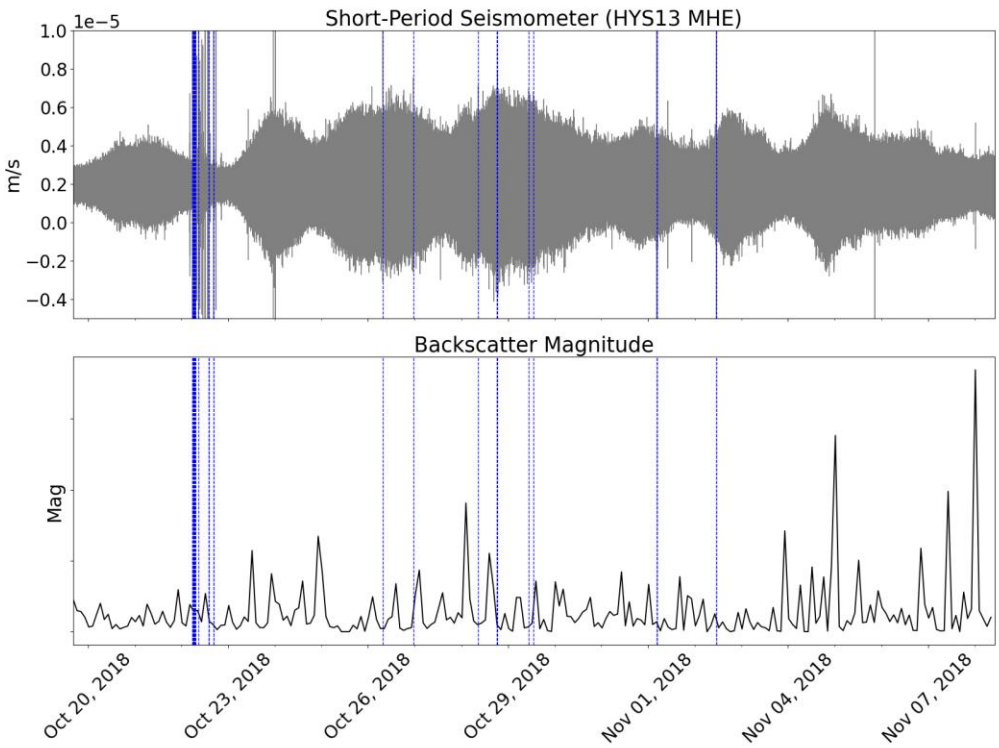

Figure S12. Bottom movements recorded by a short-period seismometer (top) and SHROS magnitude data (bottom) between 19 October and 8 November 2018. The blue lines show when high-amplitude short duration events occurred. The SDEs detected on 22 October 2018 were part of a long lasting high-amplitude tremor. Neither the detected SDEs nor the largest tremor recorded during the SHROS monitoring period (22 October 2018) coincided with heightened bubble release. The seismic plot shows the mid period MHE channel (8 Hz sample rate).

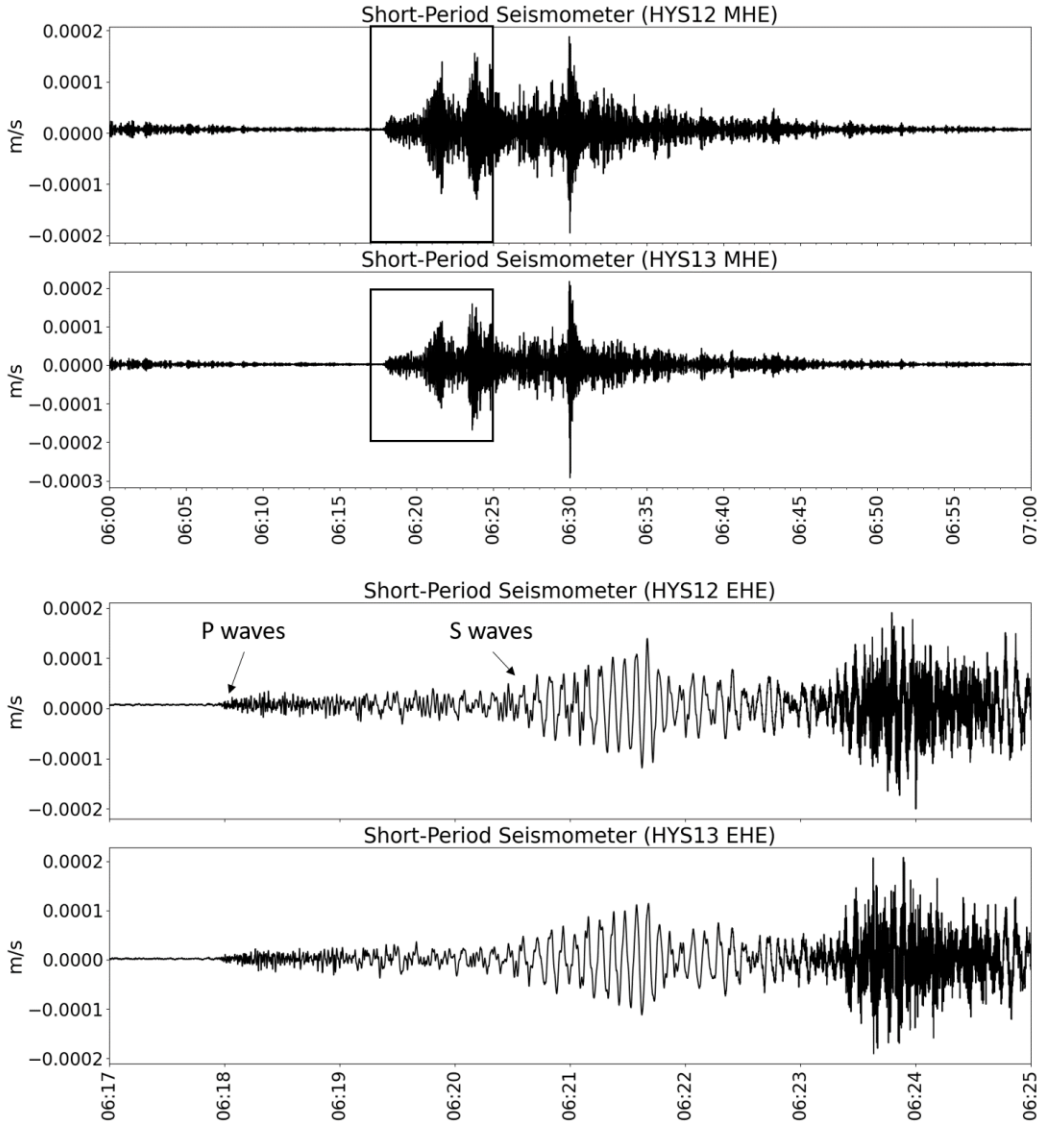

Figure S13. Bottom movements recorded by two short-period seismometers (HYS12 and HYS13) on 22 October 2018 between 6 am and 7 am, showing the largest event that was recorded during the SHROS monitoring period. The top plots show the mid period MHE channel (8 Hz sample rate) of both stations. The bottom plots show the extremely short period EHE channels (200 Hz sample rate) and focus on the start of the vibrations (black rectangles in the top plots).

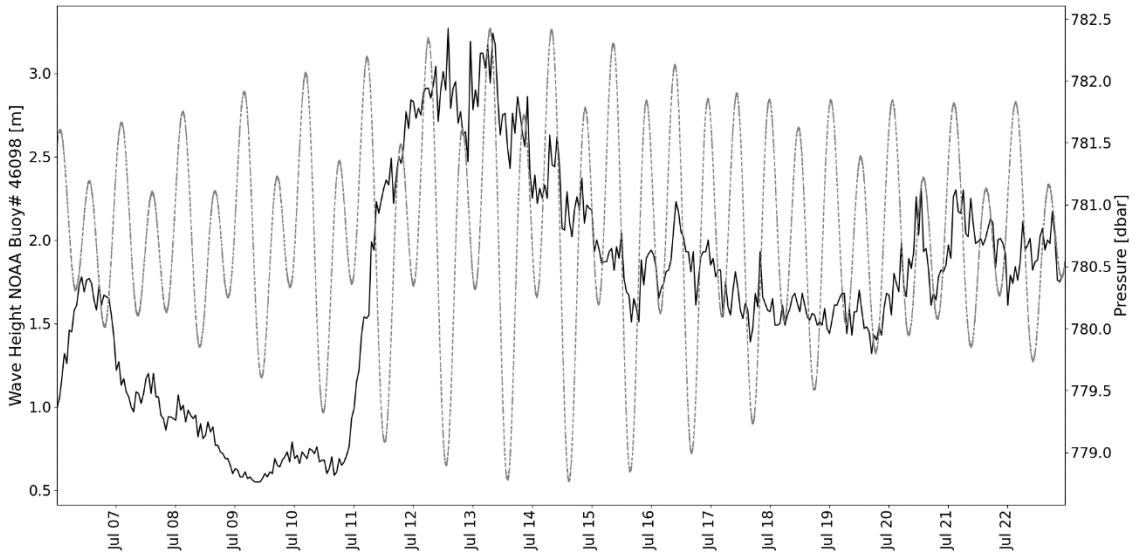

Figure S14. Wave height from the OOI-operated Buoy #46098 "OOI Waldport Offshore" plotted against the SHR bottom pressure data between 6 July and 22 July 2018.

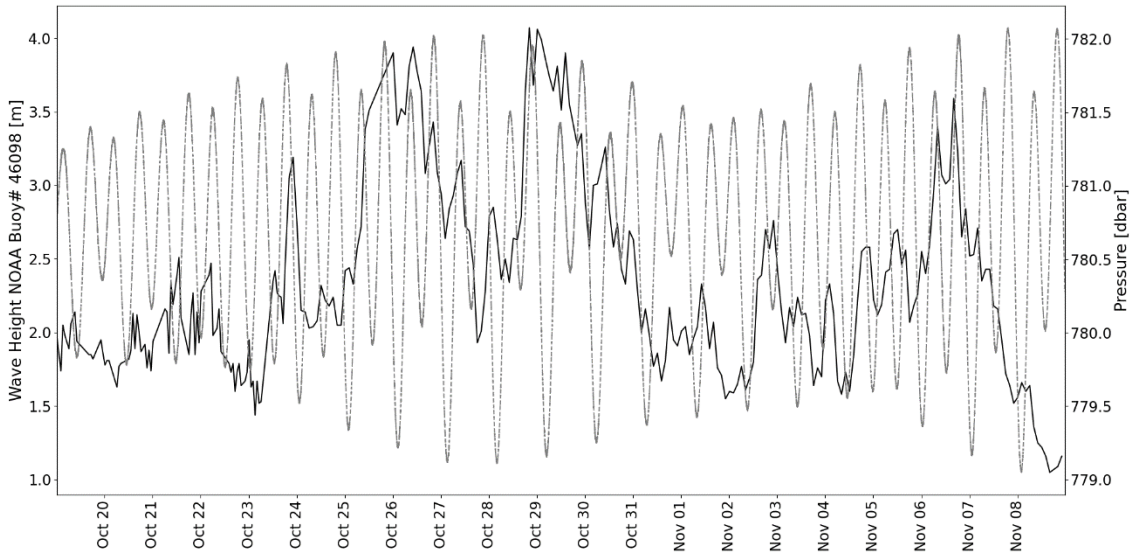

Figure S15. Wave height from the OOI-operated Buoy #46098 "OOI Waldport Offshore" plotted against the SHR bottom pressure data between 19 October and 8 November 2018.

Monitoring period (day/month)	Duration	Number of scans	Pulse length (µs)	Sound Level (dB)	Receiver Gain (dB)	Absorption (dB/km)	Relative data quality
06/07 - 22/07	15 days, 6 h	183	70	221	20	51	High SNR but wrong absorption value
22/07 - 24/07	2 days, 14 h	31					
24/07 - 26/07	1 day, 8 h	16	70	221	20	51	High SNR but wrong absorption value
26.07 - 29/07	3 days	36					
29/07 - 10/08	12 days, 20 h	154	70	221	20	75	Low SNR
10/08 - 22/08	2 days, 22 h	35					
13/08 - 22/08	8 days, 22 h	107	70	221	20	75	Low SNR
22/08 - 06/09	15 days	180					
06/09 - 13/09	7 days	84	70	221	20	75	Low SNR
13/09 - 17/09	3 days, 22 h	47					
17/09 - 18/09	1 day	12	560	221	20	75	Medium SNR
18/09 - 20/09	2 days, 4 h	26	560	212	20	75	Medium SNR, low far-range detection
20/09 - 04/10	13 days, 6 h	159					
04/10 - 05/10	1 day, 14 h	19	280	206	30	75	Low SNR, low far-range detection
05/10 - 10/10	4 days, 10 h	53	280	221	10	75	High SNR, scans limited to 245°
10/10 - 16/10	6 days, 8 h	76					
16/10 - 16/10	6 h	3	280	221	10	75	High SNR, scans limited to 245°
16/10 - 18/10	1 day, 8 h	16					
18/10 - 18/10	2 h	1	280	221	10	75	High SNR, scans limited to 245°
18/10 - 18/10	16 h	8					
18/10 - 19/10	14 h	7	280	221	10	75	High SNR, scans limited to 245°
19/10 - 19/10	8 h	4					
19/10 - 25/10	5 days, 16 h	68	280	221	10	75	High SNR, scans limited to 245°
25/10 - 25/10	8 h	4					
25/10 - 08/11	13 days, 20 h	166	280	221	10	75	High SNR, scans limited to 245°

Table S1. Operation log of the Southern Hydrate Ridge Overview Sonar. The sonar settings changed over time to improve the signal-to-noise ratio (SNR) and the ability to detect gas plumes. The gaps in the timeseries are caused by downtimes of the sonar or observatory due to maintenance or calibration work. Because of a calculation error, the absorption coefficient used until 26 July 2018 was too low, meaning that until then transmission losses were underestimated and undercompensated; this only accentuates the average magnitude

discrepancies between close and far range bubble plumes but does not affect results regarding the temporal variations.

Data Set S1. Matlab script used to automate the bubble counting on the CAMDSB103 images. The script is contained in a zipped file.

Data Set S2. Monthly plots showing the eastward, northward, and upward current velocities recorded by the cabled ADCP between 29 June 2018 and 29 February 2020. There is a plot image for each calendar month. All images are contained in a zipped file.

Data Set S3. Excel file containing the plume count and the bubble rise velocity results from the analysis of the CAMPAIA101 4K video sequences.

Movie S1. Time-lapse video sequence showing all bubble plumes detected by the SHROS (after post-processing) between 6 July and 8 November 2018. Each frame is timestamped and represents one scan of the sonar. The video file is hosted on the PANGAEA data repository (link: https://doi.pangaea.de/10.1594/PANGAEA.932619)

Movie S2. Time-lapse video sequence showing all 360° scans recorded by the single-beam scanning-sonar (QNTSRA101) during the 24-hour survey on 14-15 November 2019. Each scan image is timestamped. The video file is hosted on the PANGAEA data repository (link: https://doi.pangaea.de/10.1594/PANGAEA.932653).

Movie S3. Video file compiling timestamped photographs acquired every 30 minutes by the CAMDSB103 at the Einstein's Grotto vent in July 2018. The video shows the morphology of the Einstein's Grotto vent changes over one month. The laser pointers on the camera images are 10 cm apart. The video file is hosted on the PANGAEA data repository (link: https://doi.pangaea.de/10.1594/PANGAEA.932649).

Movie S4. Video file compiling timestamped photographs acquired every 30 minutes by the CAMPIA101 at the Summit-A vent from 28 June 2019 to 22 January 2020. The video shows how the morphology of the Summit-A vent changes over a period of almost 7 months. The measuring stick visible on the images has a diameter of 30 mm and yellow and black graduations every 19 mm. The stick is 80 cm long and is mounted on a 30 x 30 cm square base. The stick with the base is only entirely visible in the first video frame because it is rapidly buried under collapsed sediments afterwards. The video file is hosted on the PANGAEA data repository (link: https://doi.pangaea.de/10.1594/PANGAEA.932622).